Catal Lett (2008) 123:164–171
DOI 10.1007/s10562-008-9412-x

Nitric Oxide Reduction Using Hydrogen Over Perovskite Catalysts with Promotional Effect of Platinum on Catalytic Activity

Rajesh B. Biniwale · Jayshri V. Pande · Manju Dhakad · Nitin K. Labhsetwar · Masaru Ichikawa

Received: 4 December 2007 / Accepted: 22 January 2008 / Published online: 7 February 2008

Abstract The catalytic activities of strontium substituted $La_{0.7}Sr_{0.3}MnO_3$ type perovskite catalysts for NO reduction using H_2 as reducing agent has been studied, which is further improved by incorporation of Pt outside (0.1 wt.%Pt/$La_{0.7}Sr_{0.3}MnO_3$) and inside ($La_{0.7}Sr_{0.3}Mn_{0.97}Pt_{0.03}O_3$) the perovskite lattice structure. Pt shows excellent enhancement in catalytic selectivity towards N_2 when supported on the perovskite. The catalysts were characterized using thermo-gravimetric analysis (TGA), X-ray diffraction (XRD), scanning electron microscopy (SEM) and specific surface area. Catalysts evaluations were carried out using thermo-gravimetric analysis coupled with mass spectra (TG-MS).

Keywords Nitric oxide reduction · Hydrogen · Perovskite · Platinum · Reducible support

1 Introduction

The selective catalytic reduction (SCR) of oxides of nitrogen (NO_x) using ammonia as reducing agents has attracted great attention. However, slippage of ammonia to the environment is a major concern in ammonia-SCR reaction. Accordingly, the use of hydrocarbons co-existing in the flue gases or vehicle exhaust is being explored for SCR. The direct decomposition of NO and use of appropriate non-carbon-containing molecule as reducing agent becomes important because when hydrocarbons are used as reducing agent there is possibility of increase in carbon dioxide emissions. Hydrogen, which exits in the automobile exhaust, could be the candidate molecule for NO reduction and has been reported by several researchers [1–11]. It may also be possible to use the hydrogen as reducing molecule for stationary applications. Various platinum supported catalysts have been reported for NO reduction using H_2 at relatively lower temperatures [12–15].

The noble metal based three-way catalysts have been used for auto-exhaust emission reduction generally content Pt, Rh and Pd supported on refractory oxides. Rh is being the most effective for NO reduction. At lower temperatures Pt results in higher conversion of NO however the selectivity towards conversion to N_2 is poor. In view of the limited possible supply of Rh it is imperative to look at the alternate catalyst compositions to promote the activity of Pt for NO/H_2 reaction. Accordingly, addition of metal oxides as promoter or co-catalyst has been studied. Addition of metal oxides namely WO_3 and MoO_3 has been reported for improving activity of Pt catalyst for NO/CO reaction. Neiuwenhuys and co-workers have studied the effect of addition of oxides of Co and Mn to Pt catalyst for its effect on NO/H_2 reaction [11].

Perovskite is ABO_3 type oxide having rare earth metal at ‘A’ site and transition metal at ‘B’ site. With the substitutions at ‘A’ and/or ‘B’ site with different valence elements creates valences and vacancies, which helps in controlling the mechanism of a reaction. This tailoring possibility with perovskite structure has been used and several compositions have been reported for NO reduction using hydrocarbons or CO as reducing agent [16–22]. Particularly in the case of three-way catalysis for

---

R. B. Biniwale (✉) · J. V. Pande · M. Dhakad · N. K. Labhsetwar
National Environmental Engineering Research Institute,
Nehru Marg, Nagpur 440020, India
e-mail: rb_biniwale@neeri.res.in

M. Ichikawa
Catalysis Research Center, Hokkaido University,
Sapporo 001-0021, Japan

auto-exhaust emission reduction, perovskite shows activity by participation of lattice oxygen for oxidation and selectively taking oxygen from NO_x for filling back the oxygen vacancy formed. It is possible to promote the catalyst activity by using small amount of Pt in perovskite. When Pt is present either inside the perovskite structure or as co-catalyst it can promote the activity of perovskite particularly at lower temperatures.

Incorporation noble metals (Pt, Pd, Rh etc.) into the perovskite structure results in the stabilization of noble metals against sintering, volatilization and solid-state reaction with the substrate. Enhancement in activity of the perovskite can also be achieved when small amounts of noble metals are incorporated into the perovskite structure. Sorenson et al. [23] adopted this approach to use noble metal-loaded perovskites for the simultaneous reduction of NO and the oxidation of CO and un-burned hydrocarbons. These authors found the substituted multicomponent cobaltite $La_{0.6}Sr_{0.4}Co_{0.94}Pt_{0.03}Ru_{0.03}O_3$ highly active and selective for exhaust treatment from single cylinder engine. Selective reduction of NO_x (>90%) was attained in excess CO while efficient oxidation of hydrocarbons and CO was observed at the oxidizing side of the stoichiometric O_2 to fuel ratio.

Hydrogen is preferred as reducing agent for sources of NO with relatively low temperature of flue gas. Presence of hydrogen also helps in improving catalyst activity, particularly when noble metal catalysts are dispersed on reducible supports such as perovskite. Costa et al. studied 0.1 wt.% Pt supported on $La_{0.5}Ce_{0.5}MnO_3$ perovskite type material for the $NO/H_2/O_2$ reaction in the 100–400 °C range [24]. In another report 0.1 wt.% Pt supported $La_{0.7}Sr_{0.2}Ce_{0.1}FeO_3$ perovskite catalyst has been studied for the same reaction [25]. In fact, it has been shown that the $Pd/LaCoO_3$ exhibits better activity as compared to Pd/Al_2O_3. The kinetic study of $NO + H_2$ reaction over $Pd/LaCoO_3$ has been reported by Dhainaut et al. [26].

In this paper, we report the study of NO reduction using H_2 over perovskite catalyst studied using thermo-gravimetric analysis coupled with mass spectra (TG-MS). Effect of addition of Pt and the mechanism of NO/H_2 reaction is discussed. Based on the experimental data, kinetic parameters have been estimated.

2 Experimental

2.1 Catalyst Preparation by Co-precipitation Method

Co-precipitation method was used to synthesize $La_{0.7}Sr_{0.3}MnO_3$ type perovskite catalysts. Mixed salt solution was prepared by dissolving lanthanum nitrate (6.67 g), strontium nitrate (1.39 g) and manganese acetate (5.39 g), obtained from E-Merck, in 100 mL of water and stirred for 15 min. with heating at about 50 °C. NH_4OH solution about 300 mL (50% v/v) was then slowly added to the above metal solutions at a rate of 100 mL min^{-1} with stirring (100 rpm).The precipitate thus obtained was allowed to settle overnight followed by filtration with thorough washings with de-ionized water. The precipitate cake was then kept in an oven at 120 °C for 8h for drying and the resultant mass was then calcined at 450 °C for 6 h followed by grinding and further calcination at 900 °C for 8 h. The XRD pattern of the synthesized material shows a distinct pattern for $La_{0.7}Sr_{0.3}MnO_3$.

2.2 Pt-incorporation Inside the Structure

Co-precipitation method was also used to synthesize $La_{0.7}Sr_{0.3}Mn_{0.95}Pt_{0.05}O_3$. Mixed salt solution was prepared by dissolving lanthanum nitrate (6.67 g), strontium nitrate (1.39 g) and manganese acetate (5.39 g) obtained from E-Merck, in 100 mL of water and stirred for 15 min. with heating at about 50 °C. NH_4OH solution about 300 mL (50% v/v) was then slowly added to the above metal solutions at a rate of 100 mL min^{-1} with stirring (100 rpm). The precipitate cake was mixed together with addition of 50 mL hexachloroplatinic acid solution mixed thoroughly by stirring for 20 min. The slurry was then dried in oven at 120 °C for 8 h. The resultant mass was calcined at 450 °C for 6 h followed by grinding and further calcination at 900 °C for 8 h to get $La_{0.7}Sr_{0.3}Mn_{0.97}Pt_{0.03}O_3$.

2.3 Pt-impregnation Outside the Structure

$La_{0.7}Sr_{0.3}MnO_3$ catalyst was synthesized using the same procedure as described above. A catalyst with composition 0.1 wt.% $Pt/La_{0.7}Sr_{0.3}MnO_3$, was prepared by impregnating the host catalyst (5 g) with 100 mL aqueous solution of hexachloroplatinic acid containing 0.1 wt.% equivalent platinum, followed by drying at 120 °C for 4 h and calcining at 650 °C for 5 h in air.

2.4 Catalyst Characterizations

Catalysts were characterized for X-ray diffraction (XRD) and Bruaner–Emette–Tailor (BET) methods for the confirmation of perovskite phase formation and specific surface area respectively. XRD patterns were recorded on a Rigaku Rint-220HF diffractometer, operated at 40 kV and 50 mA with a monochromator and using Cu-Kα radiation ($\lambda = 0.15418$ nm). Indexing of XRD peaks was done, by using the JCPDS cards for the respective phases. Surface area was measured by nitrogen adsorption using the automatic gas adsorption apparatus BELSORP 28SA (produced by Nippon Bell Co. Japan) and evaluated by BET method. The SEM investigations were carried out by HITACHI S-5000 instrument using 10.0 kV acceleration voltages.

2.5 Catalytic Activity

The experimental setup used for the evaluation of the NO reduction over catalyst samples is shown in Fig. 1. A U-tube made up of quartz glass with 6 mm diameter was used as reactor. About 500 mg catalyst was placed in the reactor. A thermocouple was placed near catalyst bed. The entire U-tube reactor was placed in a furnace for heating. A programmable temperature controller was used to maintain the temperature of furnace. At the outlet of the reactor, a sampling probe was placed to draw sample of gas from outlet stream and fed it to mass spectroscope used for monitoring. All catalysts were cleaned by heating at 400 °C in flow of He (50 mL min^{-1}) for 6 h to remove all unwanted adsorbed species. The catalyst then was heated in the reduced atmosphere of H_2 at 450 °C for about 4 h. The each catalyst was exposed to a mixture of NO diluted in He (NO 2.11%v/v balance He) at the flow rate of 100 mL min^{-1} and H_2 at the flow rat of 2.1 mL min^{-1}. The flow rate of H_2 was maintained to keep NO:H_2 ratio at 1:1. A temperature programmed reaction method was followed. Rate of 10 °C min^{-1} was used for increasing temperature. The maximum temperature attained was 900 °C. The catalyst was heated at this temperature of 900 °C for about 25–30 min.

The formation of N_2, N_2O and NH_3 occurred in the product gas with simultaneously occurring of following reactions:

$$2NO + 2H_2 \rightarrow N_2 + 2H_2O \tag{1}$$

$$2NO + H_2 \rightarrow N_2O + H_2O \tag{2}$$

$$2NO + 5H_2 \rightarrow 2NH_3 + 2H_2O \tag{3}$$

The overall conversion of NO and H_2 to form N_2, N_2O and NH_3 was calculated using Eqs. 4 and 5 as following;

$$\tau_{NO} = \frac{2(n_{N_2} + n_{N_2O}) + n_{NH_3}}{n^0_{NO}} = \tau_{N_2} + \tau_{N_2O} + \tau_{NH_3} \tag{4}$$

$$\tau_{H_2} = \frac{2n_{N_2} + n_{N_2O} + \frac{5}{2}n_{NH_3}}{n^0_{H_2}} = \left(\tau_{N_2} + \frac{\tau_{N_2O}}{2} + \frac{5}{2}\tau_{NH_3}\right)\frac{n^0_{NO}}{n^0_{H_2}} \tag{5}$$

where, τ_i = overall conversion of component i; n_i = molar rate of component i.

Selectivity towards formation of N_2, N_2O and NH_3 was calculated using following Eqs. 6, 7 and 8

$$S_{N_2} = \frac{2r_{N_2}}{2r_{N_2O} + 2r_{N_2} + r_{NH_3}} = \frac{1}{1 + \frac{r_{N_2O}}{r_{N_2}} + \frac{r_{NH_3}}{2r_{N_2}}} \tag{6}$$

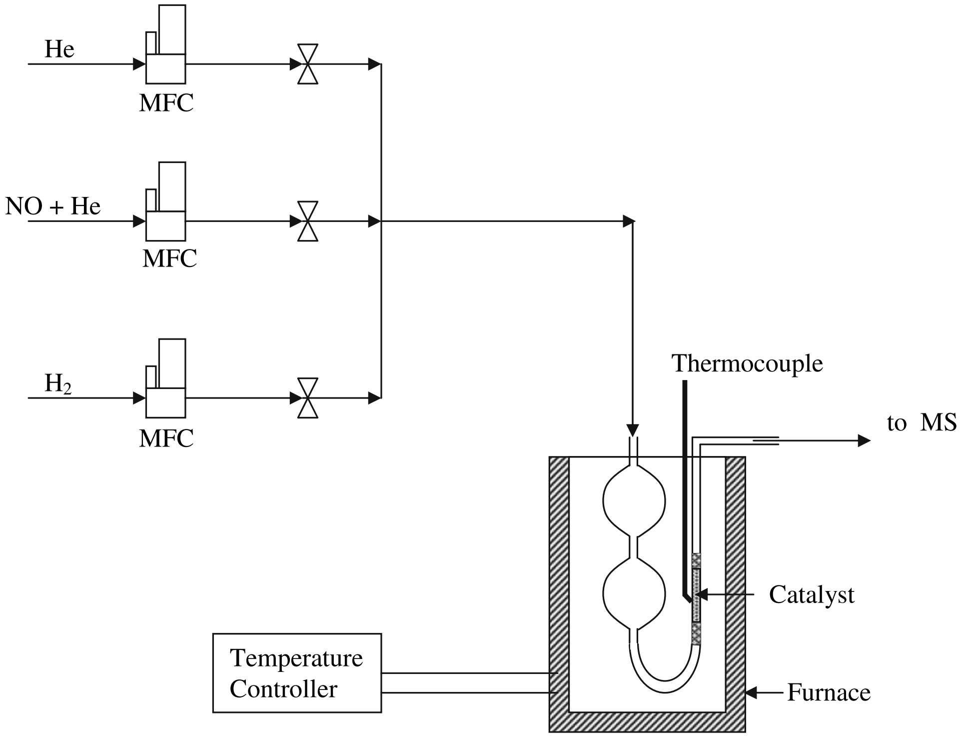

Fig. 1 Experimental setup

$$S_{NH_3} = \frac{r_{NH_3}}{2r_{N_2O} + 2r_{N_2} + r_{NH_3}} = \frac{1}{2\left(\frac{r_{N_2O}}{r_{NH_3}} + \frac{r_{N_2}}{r_{NH_3}}\right) + 1} \tag{7}$$

$$S_{N_2O} = \frac{2r_{N_2O}}{2r_{N_2O} + 2r_{N_2} + r_{NH_3}} = \frac{1}{1 + \frac{r_{N_2}}{r_{N_2O}} + \frac{r_{NH_3}}{2r_{N_2O}}} \tag{8}$$

where, r_i = rate of formation of component i; S_i = selectivity towards component i.

3 Result and Discussion

3.1 Perovskite Catalysts

The XRD pattern of the sample confirms the formation of crystalline $La_{0.7}Sr_{0.3}MnO_3$ phase with perovskite structure. The XRD patterns of $La_{0.7}Sr_{0.3}MnO_3$ catalyst shows a peak of $SrCO_3$, whose intensity increases with increasing Sr content. This infers that only a small amount of Sr could be incorporated in perovskite phase in the present synthesis. The XRD patterns for different perovskites samples used in this study are shown in Fig. 2. The XRD peaks compared to the standard data from Joint Committee on Powder Diffraction Standards (JCPDS) for the same compound JCPDS 51-0409 for $La_{0.7}Sr_{0.3}MnO_3$ were well in the agreement. A smaller amount of peaks were found for some other phases particularly strontium carbonate (JCPDS 5-418 for $SrCO_3$). This confirms the phase of sample catalyst as the perovskite. From XRD patterns in the case of $La_{0.7}Sr_{0.3}MnO_3$ and 0.1 wt.%Pt/$La_{0.7}Sr_{0.3}MnO_3$ additional peaks for $SrCO_3$ have been observed these are not significant peaks and $SrCO_3$ must be present as impurities in very small amount. These impurities are not likely to have considerable catalytic activity.

The BET surface area results are shown in Table 1. The surface area of catalytic materials even after calcination at higher temperature is in the range of 3–4.3 $m^2\ g^{-1}$. The catalysts were also characterized by using scanning electron micrograph (SEM). The SEM micrographs in Fig. 3 show that the powders obtained by co-precipitation method contain agglomerates of perovskite.

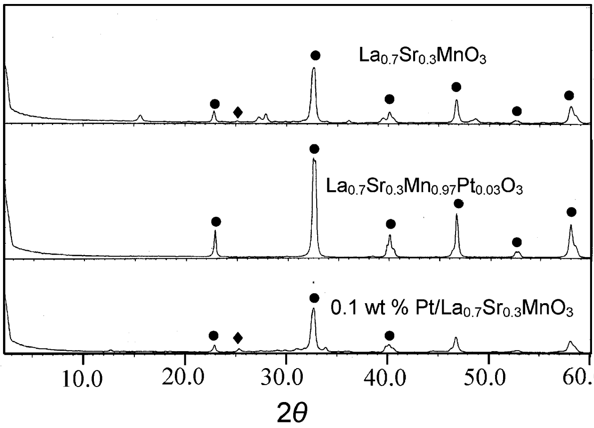

Fig. 2 XRD data of different catalysts, peaks identification ● perovskite $La_{0.7}Sr_{0.3}MnO_3$ and ◆ $SrCO_3$

Table 1 BET Surface area results of different catalyst composition

S. No.	Catalyst composition	BET surface area ($m^2\ g^{-1}$)
1	$La_{0.7}Sr_{0.3}MnO_3$	4.3
2	0.1 wt.% Pt/$La_{0.7}Sr_{0.3}MnO_3$	3.0
3	$La_{0.7}Sr_{0.3}Mn_{0.97}Pt_{0.03}O_3$	3.6

3.2 NO Reduction with H_2

A ratio of ca 1:1 for NO:H_2 was introduced as feed over catalyst pre-treated with H_2. When H_2 is present, two additional reactions can occur viz.; formation of H_2O by reaction of gaseous phase H_2 with adsorbed oxygen (reaction 2), and formation of NH_3 (reaction 3), besides reduction of NO.

A temperature-programmed reaction was carried out for reduction of NO over $La_{0.7}Sr_{0.3}MnO_3$ catalysts and the results are depicted in Fig. 4. At temperature above 350 °C the concentration of NO decreases rapidly with corresponding increases in concentrations of N_2, NH_3 and H_2O. At ca 900 °C nearly complete reduction of NO is observed with conversion of ca 99% and equilibrium turn over frequency (TOF) of $15 \times 10^{-3}\ min^{-1}$ as shown in Table 2. Under the flow of H_2 concentration of ammonia is significant during reaction over $La_{0.7}Sr_{0.3}MnO_3$ catalysts. The selectivity towards N_2 is 38.38% and towards NH_3 is 61.7%. Formation of N_2O in small concentration at about 470 °C as an intermediate product is also observed.

3.3 Effect of Pt on Reduction of NO with H_2 Over Perovskite

When reduction of NO with H_2 is carried out over $La_{0.7}Sr_{0.3}MnO_3$ doped with 0.1 wt.% Pt, reaction occurred very rapidly at temperature of ca 300 °C. The observed change in concentration of products is reported in Fig. 5. At lower temperature of 200 °C, peak-decrease in concentration of NO is observed which possibly correspondence to oxidation of reduced perovskite using NO. Concentration of NO is decreased from 35 mol% at ca. 185 °C to 32 mol% at 200 °C. Subsequently increases to 35 mol% again at ca 240 °C. Further increase in temperature to 275 °C leads to reduction of NO with H_2 with a

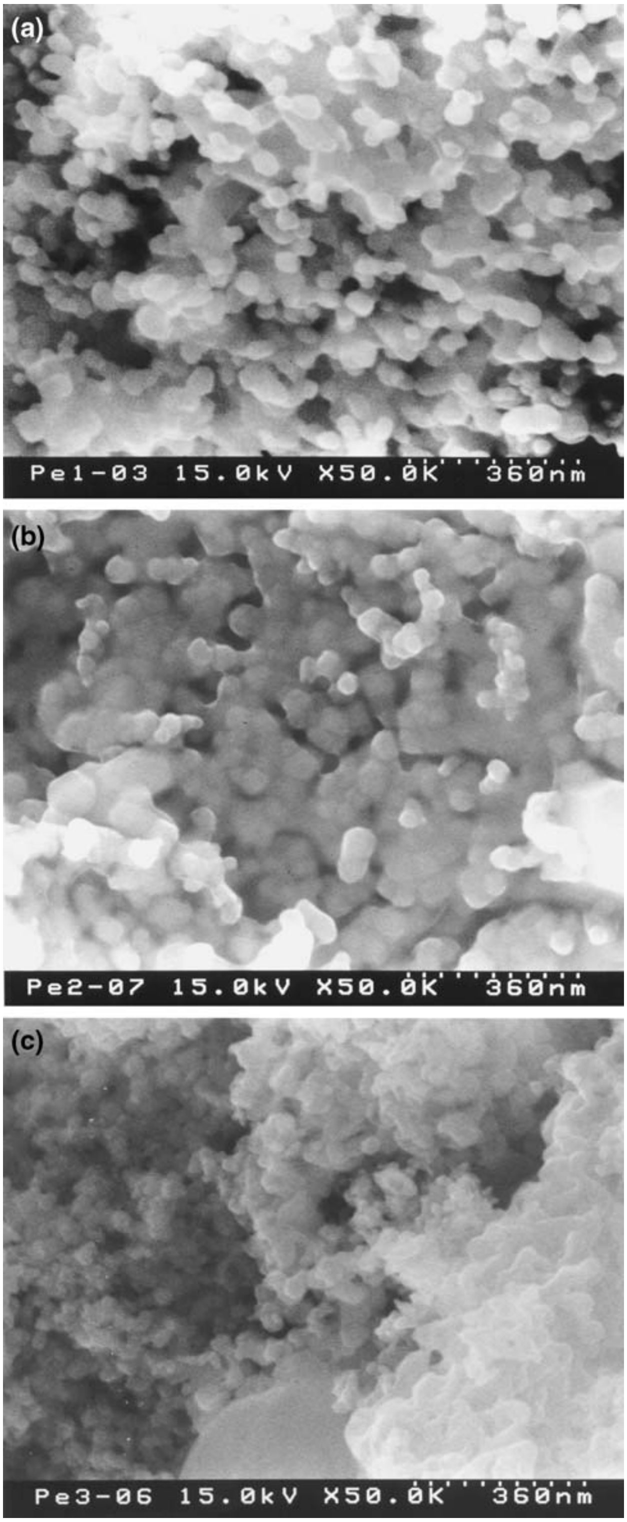

Fig. 3 SEM data of different catalysts, (**a**) $La_{0.7}Sr_{0.3}MnO_3$, (**b**) 0.1 wt.% Pt/$La_{0.7}Sr_{0.3}MnO_3$, and (**c**) $La_{0.7}Sr_{0.3}Mn_{0.97}Pt_{0.03}O_3$

rapid rate. The conversion of NO is 99.6% at ca 310 °C and concentration of N_2 is observed to be about 18%. The TOF at equilibrium is about 21.1 × 10^{-3} min^{-1}. The selectivity towards N_2 is observed to be improved to 63.26% in presence of Pt as shown in Table 2. The concentrations of N_2 and NH_3 were observed to be oscillating during the course of reactions this may be due to catalytic reduction of NO using NH_3 on Pt catalysts.

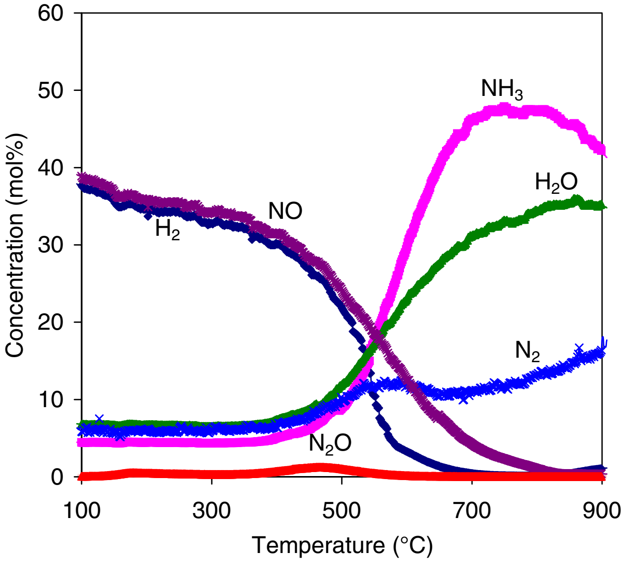

Fig. 4 NO reduction with H_2 over $La_{0.7}Sr_{0.3}MnO_3$

Results obtained during reduction of NO over $La_{0.7}Sr_{0.3}Mn_{0.97}Pt_{0.03}O_3$ are shown in Fig. 6. Decrease in concentration of NO observed is with rapid rate in initial stages when temperature is 100–150 °C unlike the case with Pt doped perovskite catalysts. A peak is observed at ca 165 °C, which may be for oxidation of reduced perovskite. At higher temperatures with slower rate NO concentration decreases to zero at ca 485 °C. Selectivity towards N_2 observed to be lower than Pt existing outside structure of perovskite and is 52.64%. The TOF at equilibrium is about 20.4 × 10^{-3} min^{-1}.

Co-existing Pt is more effective in carrying out reduction of NO to N_2. At lower temperatures, Pt may promote reaction (2) thus showing increase in N_2O concentration. In flow of hydrogen, Pt may be in reduced state and more active therefore leads to complete conversion of NO. In addition, the reduced Pt is expected to exhibit activity for NO reduction with NH_3. From selectivity data on different catalysts it may be concluded that the N_2 selectivity increase when perovskite is combined with Pt in both cases i.e., Pt outside the perovskite structure or incorporated within.

For comparison of incorporation of other promoter metals both inside and outside perovskite structure the research work is under progress. In case of the 0.1 wt.% Rh/$La_{0.7}Sr_{0.3}MnO_3$ selectivity towards N_2 is relatively higher at about 76.2% and the TOF at equilibrium is about 25.2 × 10^{-3} min^{-1} however the conversion observed was

Table 2 NO Reduction with H_2 over various catalysts

Catalyst composition	Conversion[a] (%)	N_2 Selectivity[a] (%)	NH_3electivity[a] (%)	TOF[a] (10^{-3} min^{1})
$La_{0.7}Sr_{0.3}MnO_3$	99.1	38.38	61.7	15.0
0.1 wt.%Pt/$La_{0.7}Sr_{0.3}MnO_3$	99.6	63.26	36.7	21.1
$La_{0.7}Sr_{0.3}Mn_{0.97}Pt_{0.03}O_3$	99.5	52.64	47.9	20.4

[a] Estimated at equilibrium at 900 °C

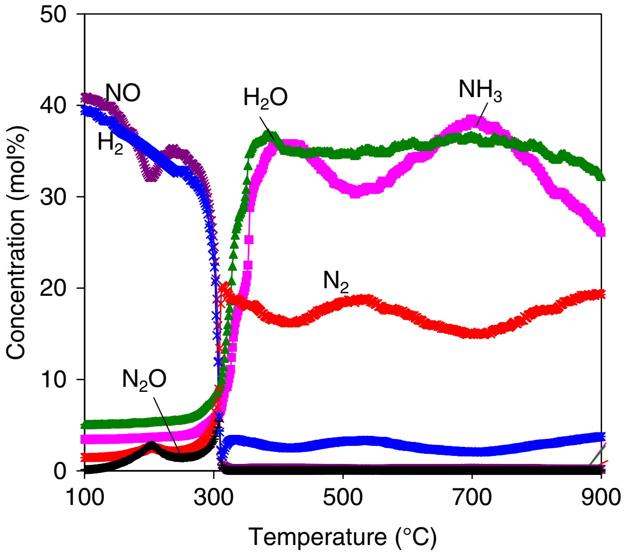

Fig. 5 NO reduction with H_2 over 0.1 wt.% Pt/$La_{0.7}Sr_{0.3}MnO_3$

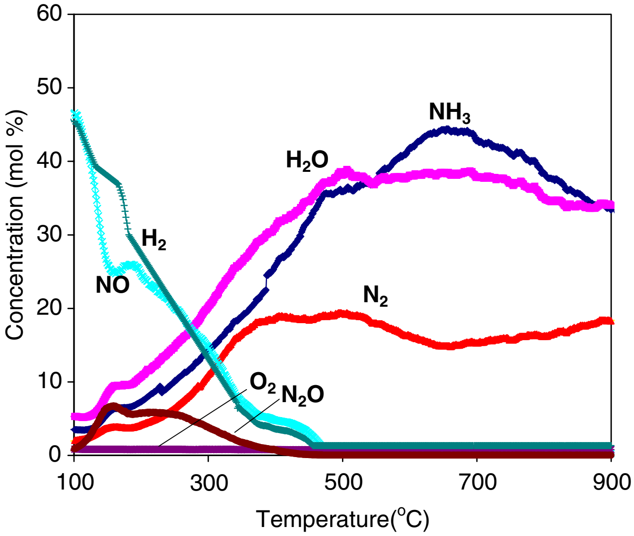

Fig. 6 NO reduction with H_2 over $La_{0.7}Sr_{0.3}Mn_{0.97}Pt_{0.03}O_3$

lower at about 12%. More data on effect of various different promoters will be discussed later.

3.4 Reaction Rate Estimations

The rate of reactions has been estimated for all three catalysts under the reaction conditions as specified in experimental section. Apparent activation energies for the overall NO transformations were calculated using Arrhenius equation for NO and H_2 conversion. The estimated values of apparent activation energies are reported in Table 3. The activation energies for $La_{0.7}Sr_{0.3}MnO_3$ and 0.1 wt.% Pt/$La_{0.7}Sr_{0.3}MnO_3$ catalysts are in the range of 13.36–19.49 kJ mol^{-1}. Whereas, in the case of $La_{0.7}Sr_{0.3}Mn_{0.97}Pt_{0.03}O_3$ catalysts, the activation energy for NO and H_2 conversion are 25.5 and 40.63 kJ mol^{-1}. These are much higher as compared to other two catalysts used in this study. The apparent reaction orders were estimated by nonlinear regression analysis using sequential quadratic programming in SPSS 7.5.1. The negative reaction orders obtained indicates the inhibiting effect on the reaction rates.

3.5 Kinetics of NO Reduction Over Perovskite

The kinetics of NO reduction with H_2 is reported by a few researchers as compared to most of the studies reporting kinetics of NO reduction with CO. In view of the importance of using H_2 as reducing agent the kinetics of the reaction over Pt supported on metal oxides has been discussed for possible hydrogen assisted dissociation of NO or formation of N_2O as intermediate while reducing NO to N_2 [27, 28]. The mechanisms reported are Langmuir–Hinshelwood or Eley–Rideal mechanism. When reducible support such as mixed oxides or perovskites is used for dispersion of noble metal, more active sites are formed by reduction of 'B' site metal of perovskite. This results in enhancement in selectivity towards N_2.

Mechanism involving competitive adsorption of NO and H_2 along with a dissociation step for NO is generally proposed for noble metal catalysts. The mechanism involve following steps [27];

$$NO + * \leftrightarrow NO_{(a)} \quad (9)$$

$$H_2 + 2* \leftrightarrow 2H_{(a)} \quad (10)$$

$$NO_{(a)} + H_{(a)} \leftrightarrow N_{(a)} + OH_{(a)} \quad (11)$$

$$N_{(a)} + N_{(a)} \leftrightarrow N_2 + 2* \quad (12)$$

$$NO_{(a)} + N_{(a)} \leftrightarrow N_2 + O_{(a)} + * \quad (13)$$

Table 3 Activation energies and order of reaction for conversion of NO and H_2 during NO + H_2 reaction

Catalyst	ENO[a] (kJ mol^{-1})	EH_2^b (kJ mol^{-1})	P_{NO} (10^{-3} atm)	P_{H_2} (10^{-3} atm)	*m*	*n*
$La_{0.7}Sr_{0.3}MnO_3$	18.28	15.73	3.8–390	10.2–378	−0.152	−0.15
0.1 wt.%Pt/$La_{0.7}Sr_{0.3}MnO_3$	19.49	13.36	1.7–421	37–408	−0.283	−0.243
$La_{0.7}Sr_{0.3}Mn_{0.97}Pt_{0.03}O_3$	25.5	40.63	21.4–504	13–492	−0.052	−0.531

[a] Estimated using $r_{NO} = A_{NO}\exp(-E_{NO}/RT)p_{NO}^m p_{H_2}^n$

[b] Estimated using $r_{H_2} = A_{H_2}\exp(-E_{H_2}/RT)p_{NO}^m p_{H_2}^n$

$$NO_{(a)} + N_{(a)} \leftrightarrow N_2O + 2* \quad (14)$$

$$N_{(a)} + H_{(a)} \leftrightarrow NH_{(a)} + * \quad (15)$$

$$NH_{(a)} + H_{(a)} \leftrightarrow NH_{2,(a)} + * \quad (16)$$

$$NH_{2,(a)} + H_{(a)} \leftrightarrow NH_3 + 2* \quad (17)$$

$$O_{(a)} + H_{(a)} \leftrightarrow OH_{(a)} + * \quad (18)$$

$$OH_{(a)} + H_{(a)} \leftrightarrow H_2O + 2* \quad (19)$$

The rate of NO conversion into N_2, N_2O and NH_3 can be given as Eq. 20

$$r_{NO} = 2(r_{N_2O} + r_{N_2}) + r_{NH_3} = 2(r_{14} + r_{12} + r_{13}) + r_{17} \quad (20)$$

with $r_{15} = r_{16} = r_{17}$ under steady-state conditions and

$$r_{12} = k_{12}\theta_N^2 \quad (21)$$

$$r_{13} = k_{13}\theta_{NO}\theta_N \quad (22)$$

$$r_{14} = k_{14}\theta_{NO}\theta_N \quad (23)$$

$$r_{15} = k_{15}\theta_N\theta_H \quad (24)$$

where, k_n = the rate constant related to step n; θ_i = coverage of adsorbate i.

Dhainaut et al. have discussed the detail mechanism for NO reduction with H_2 over Pd/Al_2O_3 and Pd/$LaCoO_3$ catalysts [26]. As reported the hydrogen adsorption could be a limiting step when Pd/$LaCoO_3$ catalyst is considered. Probability of finding two adjacent sites for the dissociative adsorption of H_2 on Pd is very low due to high NO coverage. In fact, studies conducted by H_2/D_2 exchange on Pd monolith confirm that the hydrogen is adsorbed as precursor molecule on single site of Pd. Beutl et al. [29] also supported the involvement of adsorbed molecular hydrogen. Based on this discussion NO reduction with H_2 over reducible support is reported to involve Langmuir–Hinshelwood mechanism with reaction sequence as follows:

$$NO + * \leftrightarrow NO_{(a)} \quad (9)$$

$$H_2 + * \leftrightarrow H_{2(a)} \quad (25)$$

$$NO_{(a)} + H_{2(a)} \leftrightarrow NH_{(a)} + OH_{(a)} \quad (26)$$

$$NO_{(a)} + NH_{(a)} \leftrightarrow N_2 + OH_{(a)} + * \quad (27)$$

$$NO_{(a)} + NH_{(a)} \leftrightarrow N_2O + H_{(a)} + * \quad (28)$$

$$NH_{(a)} + H_{2(a)} \leftrightarrow NH_3 + 2* \quad (29)$$

$$OH_{(a)} + H_{(a)} \leftrightarrow H_2O + 2* \quad (19)$$

Mechanism of NO reduction with H_2 on supported Pt catalysts has been reported by Shestov et al. [30] Involving two different routes for N_2 production namely either through interaction of two equivalent species or interaction of weakly adsorbed NO with NO-derived species. Considering the reports on rate expression for Pt and Pd catalysts following expression was adopted for this study for estimating kinetic and thermodynamic parameters for 0.1 wt.% Pt/$La_{0.7}Sr_{0.3}MnO_3$ and $La_{0.7}Sr_{0.3}Mn_{0.97}Pt_{0.03}O_3$ catalysts.

$$r_{NO} = \frac{2k_{26}\lambda_{NO}\lambda_H p_{NO} p_{H_2}}{(1 + \lambda_{NO}p_{NO} + \lambda_{H_2}p_{H_2})^2} \quad (30)$$

where, λ_i = equilibrium constant for component I, atm^{-1}. p_i = partial pressure of component i.

In the case of $La_{0.7}Sr_{0.3}MnO_3$ catalyst the above equation do not fit well and thus a modified equation as following was considered for estimating kinetic parameters.

$$r_{NO} = \frac{2k_{26}\lambda_{NO}p_{NO}}{(1 + \lambda_{NO}p_{NO} - \lambda_{H_2}p_{H_2})^2} \quad (31)$$

The kinetic parameters estimated using sequential quadratic programming method are reported in Table 4. The equations used for kinetic parameter estimations were (30) and (31). The results indicate that the NO adsorbs more strongly as compared to H_2. This is in agreement with earlier reported kinetic studies for Pd/$LaCoO_3$. It may be deduced that the reported mechanism is valid for the catalysts used in present study i.e., Pt supported on reducible support such as perovskite or incorporation of Pt inside the perovskite structure.

Table 4 Adjustment of the kinetic and thermodynamic constants for the NO + H_2 reaction on various catalysts

Catalyst	k[a] (m mol g^{-1} h^{-1})	λ_{NO} (atm^{-1})	λ_{H_2} (atm^{-1})
$La_{0.7}Sr_{0.3}MnO_3$	21	80	7.2
0.1 wt.%Pt/$La_{0.7}Sr_{0.3}MnO_3$	97	500	10
$La_{0.7}Sr_{0.3}Mn_{0.97}Pt_{0.03}O_3$	17	72	34.8

[a] k from Eq. 26, k_{26}

4 Conclusion

Reduction of NO over strontium substituted lanthanum magnetite perovskite type of catalysts has been carried out. Reduction of NO occurs on perovskite reduced by pretreatment under H_2 flow. The catalytic activity is further enhanced in terms of activity at lower temperature when Pt is incorporated inside the structure of perovskite. This may be due to close contact between active sites on perovskite surface and active metal sites. Excellent improvement in selectivity towards N_2 was observed by incorporation of Pt. Kinetic parameters estimation exhibits strong adsorption of NO and its reaction with adsorbed H_2.

References

1. Rausenberger B, Swiech W, Schmid AK, Rastomjee CS, Emgel W, Bradshaw AM (1998) J Chem Soc Faraday Trans 94(7):963
2. Dumpelmann R, Cant NW, Trimm DL (1994) In: Frennet A, Bastin J-M (eds) 3rd ICC and automotive pollution control, brussels, vol 2. Universit'e Libre De Bruxelles, Brussels, Belgium, p. 13
3. Tomishige K, Asakura K, Iwasawa Y (1995) J Catal 157:472
4. Hecker WC, Bell AT (1985) J Catal 92:247
5. Hornung A, Muhler M, Ertl G (1998) Catal Lett 53:77
6. Kobylinski TP, Taylor BW (1974) J Catal 33:376
7. Huang SJ, Walters AB, Vannice MA (1998) J Catal 173:229
8. Burch R, Scire S (1994) Catal Lett 27:177
9. Salama TM, Ohnishi R, Shido T, Ichikawa M (1996) J Catal 162:169
10. Tanaka T, Yokota K, Doi H, Sugiura M (1997) Chem Lett 273
11. Ferri D, Forni L, Dekkers MAP, Nieuwenhuys BE (1998) Appl Catal B: Environmental 16:339
12. Frank B, Emig G, Renken A (1998) Appl Catal B: Environmental 19:45
13. Burch R, Coleman MD (1999) Appl Catal B: Environmental 23:115
14. Ueda A, Nakao T, Azuma M, Kobayashi T (1998) Catal Today 45:135
15. Yokota K, Fukui M, Tanaka T (1997) Appl Surf Sci 121/122:273
16. Mizuno N, Yamato M, Tanaka M, Misono M (1989) Chem Mater 1:232
17. Chien MW, Pearson IM, Nobe K (1978) Ind Eng Chem Prod Res Dev 70:100
18. Mizuno N, Tanaka M, Misono M (1992) J Chem Soc Faraday Trans 88:91
19. Lindsteld A, Stromberg D, Milh MA (1994) Appl Catal 116:109
20. Teraoka Y, Nii H, Kagawa S, Jansson K, Nygren M (1996) Chem Lett 323
21. Simonot L, Garin F, Maire G (1997) Appl Catal B: Environmental 11:181
22. Forni L, Oliva C, Vatti FP, Kandala MA, Ezerets AM, Vishniakov AV (1996) Appl Catal B: Environmental 7:269
23. Sorenson SC, Wronkiewicz JA, Sis LB, Wirtz GP (1974) Ceram Bull 53:446
24. Costa CN, Stathopoulos VN, Belessi VC, Efstathiou AM (2001) J Catal 197:350
25. Costa CN, Savva PG, Andronikou C, Lambrou PS, Polychronopoulou K, Belessi VC, Stathopoulos VN, Pomonis PJ, Efstathiou AM (2002) J Catal 209:456
26. Dhainaut F, Pietrzyk S, Granger P (2007) Appl Catal B: Environmental 70:100
27. Shestov AA, Burch R, Sullivan JA (1999) J Catal 186:362
28. Burch R, Coleman MD (2002) J Catal 2058:435
29. Beutl M, Lesnik J, Rendulic KD, Hirschl R, Eichler A, Kresse G, Hafner J (2001) Chem Phy Lett 342:473
30. Burch R, Shestov AA, Sullivan JA (1999) J Catal 186:353